Observation of a nuclear-elastic-scattering effect caused by energetic protons on deuteron slowing-down behaviour on the Large Helical Device

Observation of a nuclear-elastic-scattering effect caused by energetic protons on deuteron slowing-down behaviour on the Large Helical Device

H. Matsuura, S. Sugiyama, K. Kimura, S. Kajimoto, T. Nishitani, K. Ogawa, Y. Kawamoto, M. Isobe, and M. Osakabe

1. What are the new results or developments reported in your article?

A first attempt to observe a nuclear-elastic-scattering (NES) effect caused by energetic protons on deuteron slowing-down behaviour was made on the Large Helical Device located at the National Institute for Fusion Science.

2. In what way are these new results or developments timely?

The nuclear scattering appears in usual nuclear burning plasma, in some cases, bringing this process into competition with the Coulombic scattering process. The effect may be more important for large fusion devices which has high-energy beams, i.e., in the order of 1 MeV. The fusion community is now progressing to unexplored scenarios (DT nuclear burning plasma achievement on ITER device). In reactor plasma MeV-order ions play important role for plasma sustainment, and in such a plasma effect of nuclear force would be appreciable in collisional interaction. The result, finding in this paper is timely for full-scale plasma experiment with nuclear burning.

3. Why are these new results or developments significant?

This process is very important for future nuclear fusion systems, i.e., DEMO reactor and D-^{3}He fusion reactor. For example, transferred power ratio from energetic protons to bulk ions is predicted to be increased almost 10 % in DEMO and more than 3 times in D-^{3}He reactors. However, the experimental validation has not been well made, especially for macroscopic (collective) effect on plasma.

Observation of a nuclear-elastic-scattering effect caused by energetic protons on deuteron slowing-down behaviour on the Large Helical Device

by

H. Matsuura[1], S. Sugiyama[1], K. Kimura[1], S. Kajimoto[1],

T. Nishitani[2], K. Ogawa[2,3], Y. Kawamoto[2], M. Isobe[2,3], and M. Osakabe[2,3]

[1]Department of Applied Quantum Physics and Nuclear Engineering,
Kyushu University, 744 Motooka, Fukuoka 819-0395, Japan
[2]National Institute for Fusion Science, National Institutes of Natural Sciences,
322-6 Oroshi-cho, Toki 509-5292, Japan
[3]SOKENDAI (The Graduate University for Advanced Studies),
322-6 Oroshi-cho, Toki 509-5292, Japan

Corresponding author: H. Matsuura (e-mail: mat@nucl.kyushu-u.ac.jp)

(Dated: 16 February 2020)

Abstract

A first attempt to observe a nuclear-elastic-scattering (NES) effect caused by energetic protons on deuteron slowing-down behaviour was made on the Large Helical Device located at the National Institute for Fusion Science. The NES effect on fast-ion slowing-down property can have influence on fast-ion confinement property, ion heating, fusion reaction rate coefficient, etc. An intense hydrogen beam was injected into a deuterium plasma to create a knock-on tail, i.e., a non-Maxwellian energetic component in the deuteron velocity distribution function. We conducted two types of experiment, i.e., (1) observation of the knock-on tail slowing-down property and (2) observation of the NES effect on fast-ion slowing down time. The phenomena are discussed in terms of the difference in the decay process of the $D(d,n)^3He$ neutron generation rate after neutral beam heating is terminated between the cases when the knock-on effect is influential and not influential, and also from the difference in the neutron decay times. The results of a series of experiments indicate that the NES effect caused by energetic protons can have an impact on fast-deuterons slowing-down process.

Prepared for submission to Nuclear Fusion

1. Introduction

In a thermonuclear plasma, energetic ions are continuously produced, and they play important roles in sustaining the process of plasma burning. Nuclear elastic scattering (NES) [1] contributes to the deceleration of energetic ions. The cross section of NES is defined by subtracting Coulomb scattering contribution from the experimentally measured one [1]. NES is a non-Coulombic scattering process, and a large fraction of ion energy is transferred in a single scattering event. NES always occurs in plasma operations and experiments, and it can introduce an additional energy-transfer channel between ions, in some cases, bringing this process into competition with the Coulombic scattering process. In deuterium-tritium (DT) plasma, the NES effect on the properties of plasma burning may be small [2, 3]. However, the NES effect will still be observed during usual plasma operations, for example, in the neutron emission spectrum as a result of the $T(d,n)^4He$ reactions [4]. Ryutov [5] has indicated that the NES of α-particles significantly affects the distribution function of the impurity ions, and the phenomenon may be utilized to perform plasma diagnostics. The formation of a knock-on tail in deuteron and triton distributions by α-particles and its effect on the emitted-neutron spectrum were examined by Fisher [6] and Ballabio [4]. Energetic neutron generation due to knock-on deuterons has been ascertained in JET experiment [7,8]. On the contrary, in deuterium-helium-3 (D^3He) plasma, the NES effects caused by energetic protons (produced by $^3He(d,p)^4He$ reactions) can be an important physical phenomena that contribute to the feasibility of D^3He plasma [9,10]. Many estimations of D^3He plasma have indicated that the transferred power ratio from energetic protons to bulk ions is enhanced by approximately three-fold due to NES compared to the case in which only the energy transfer via Coulomb collisions is considered [9]. In such a situation, the $n\tau$ confinement parameter can be significantly reduced [10]. At this point, however, no experiments have been carried out to quantitatively exhibit the NES effect on plasma performance as a collective phenomenon that is induced by the energetic ions in high-temperature plasmas. To ensure the fusion reactor development, it is important to experimentally observe and validate this phenomenon using

the relevant numerical models.

As an initial step, this paper reports on an experiment to observe the NES effect by the externally injected protons on slowing-down behaviours of fast deuterons. The experiment was conducted using the Large Helical Device (LHD) at the National Institute for Fusion Science (NIFS) [11].

2. Experimental apparatus and property of knock-on tail

Figure 1 depicts a schematic of the set of neutral beam injectors (NBIs) in the LHD. In the experiment, deuterium plasma is used, and the deuterium plasma was heated by NBIs and electron cyclotron resonance heating (ECH). We prepared two types of negative-hydrogen (H) beams (a) NBI#1 and 3, and (b) NBI#2, and positive-deuterium (D) beam (NBI#4 and 5) injectors. NBI#1, 2, and 3 are injectors that are directed tangentially toward the axis of the toroidal magnetic field, with the negative-ion sources providing fast particles at energy of 180 keV. NBI#4 and 5 are perpendicular to the magnetic axis, with positive-ion sources with energies of 60 and 80 keV, respectively. The two tangential NBIs are H beams in which ~1% deuterium is included as an impurity (NBI#1 and 3), and the other tangential H beam includes D as from natural abundance (N/A), i.e., ~0.015%, deuterium is included (NBI#2). The properties for NB injectors are summarized in Table 1.

The NES cross section is known to be approximately isotropic over the scattering angle in the center-of-mass system. It implies that large fraction of energy is transferred in a single scattering event compared with the Coulomb one. It is well known that in usual Fokker-Planck (FP) analysis we cannot treat such a discrete (large-angle scattering) energy-transfer process. In order to consider such a process, we introduce the Boltzmann collision term in the FP analysis [2, 3]. Although the Boltzmann collision term can also treat the small angle scattering process, we have added the Boltzmann term separately in addition to the FP term. This is because to remain the excellent technique for conventional FP method developed in this field, and the Coulomb and NES cross sections are defined separately. In

this paper we use the two types of the analysis model, i.e. Boltzmann–Fokker–Planck (BFP) and FP analysis models. The BFP simulation implies that we consider the both Coulomb scattering and NES contributions. On the other hand, the FP simulation implies we only consider the Coulomb scattering, i.e. the NES term is neglected. The BFP simulations [2, 3] for a typical plasma condition (T_i = 3 keV, T_e = 6 keV, and n_e = 0.5 × 10^{19} m^{-3}) predict that when more than ~0.1% of the deuterons are included in the H beam, the knock-on tail is buried under the beam-injected deuterons as shown in **Fig. 2**. Further, when more than ~0.1% deuterium beam (NBI#1 or 3) is used, the neutrons are produced mainly by the D(d,n)^{3}He reactions between the slowing-down beam component (blue line) and the thermal deuterons. However, when the N/A deuterons are included (NBI#2), a knock-on tail appears in deuteron distribution function, and the neutrons are mainly produced by the D(d,n)^{3}He reactions between the knock-on component (solid red line) and thermal deuterons. The D(d,n)^{3}He fusion cross-section is indicated on the same plane as the function of deuteron energy in a laboratory system. The cross-sections for NES and the D(d,n)^{3}He reaction can be observed from the results by Perkins and Cullen [12] and Bosch and Hale [13], respectively. In this paper we have neglected influence of the beam-beam fusion [14].

The decay curve of fusion-produced neutron rate is strongly dependent on the energy range of the dominant deuterons that are involved in neutron production, i.e., the D(d,n)^{3}He reaction. As depicted in **Fig. 2**, when NBI#1 or 3 was used, the 180-keV deuterons that are injected into the plasma are observed to dominate for the D(d,n)^{3}He reaction (DD neutron generation). On the other hand, if NBI#2 is used, approximately 40−100 keV deuterons produced by the knock-on of thermal deuterons via NES are dominant for the D(d,n)^{3}He reaction. The FP simulation assuming a one-dimensional velocity space in a uniform plasma, predicts that the decay of the neutron production rate is faster for a low-energy beam, compared to a high-energy beam. The difference occurs because the Coulombic scattering frequency increases with a decrease of the relative velocity v_r between the beam and bulk deuterons (with $\propto 1/v_r^4$ scaling as shown in the Rutherford differential cross-section), and

also the gradient of the D(d,n)^{3}He cross-section, i.e., $d\sigma_{DD}/dE$, is larger in the ~60-keV energy range compared to the ~180-keV range (see **Fig. 2**). When the beam energy is lower, the distribution function reaches a quasi-thermal equilibrium state faster, and the decay speed rapidly decreases. As an example, in **Fig. 3**, the decay process of the normalized neutron generation rates after the termination of the 60 and 180 keV deuterium beam are compared. The generation rates are obtained by the FP simulation and normalized to the value when the beam is terminated, i.e, t=0. The plasma condition is the same as **Fig. 2.** We can see the difference in the neutron decay features (not only the initial neutron decay time but also the total decay process until decay speed becomes sufficiently reduces) as described above.

3. Results of experiments

3.1 Observation of slowing-down feature of the knock-on tail

From the above discussion it is found that we can produce two plasma situations in experiment, i.e., where knock-on tail appears and not appear, by using the NBI#1,3 and NBI#2. By comparing the neutron attenuation curves between the two situations, we can examine the slowing-down property of the knock-on tail. In the experiment, after a period of 3.8 s from the beginning of the plasma discharge, deuterium beam injection (NBI#5) was terminated, whereas the hydrogen beam containing a small amount of deuterium (NBI#1, 2 or 3) was terminated at 4.3 s. To exclude the influence of the DT neutrons caused by triton burning on the decay curve, we chose a 0.5 s interval between the deuterium and hydrogen beam terminations. Because the knock-on tail is completely buried under the beam deuterons supplied by NBI#5 (100% deuterium beam) from 3.8 to 4.3 s, we focused our attention on the decay processes of the neutron generation rates that are observed after 4.3 s (neutrons produced by the D(d,n)^{3}He reactions between the ~180 keV deuterium component contained in the hydrogen beam (NBI#1, 2, or 3) and bulk deuterons). Based on the neutron generation rates that could be observed from more than 20 LHD shots, we estimated that approximately 1% (more than 0.1%) of the deuterons were contained in the NBI#1 and 3 hydrogen beams. In **Fig. 4**, the time variation of

the measured neutron generation rates with NBI#1 (#136131(a)) and NBI#2 (#136113(b)) are presented (comparison with the case when no additional beam was injected is made later). In this figure, the neutron generation rates are measured using the fission chamber [15]. Firstly, we notice that the gradient of the neutron generation rates gradually relaxes after 3.8 s toward each stagnation point, which indicates that a detectable number of deuterons is included in NBI#1 and 2 beams. At this point, i.e., right after the NBI#5 termination, knock-on tail is completely buried under the beam deuteron. After 4.3 s, a difference is observed in the gradient of the decay process between the NBI#1 and 2 cases. In **Fig. 5**, the normalized neutron generation rates for #136131 (NBI#1) and #136113 (NBI#2) after 4.3 s are presented and compared. The normalization was made by using the neutron generation rate at 4.3 s, thus initial values of the both curves are unity. The neutron generation rates as measured by the ^{10}B counter are presented for NBI#2 because the count rates are small (sensitivity of the ^{10}B counter is ~60 times larger compared with the FC in 10^{11} n/s range [15]). The normalized neutron generation rate for NBI#2 gradually decreases and intersects the neutron generation rate for NBI#1 at ~4.8 s. The solid lines obtained by the moving average fitting are marked on the same plane. Here the moving average is the method that we draw a viewgraph choosing the mean of an equal number of data on either side of a central value. As predicted theoretically (see Fig.3), the decay of the neutron generation rate is observed to be faster and reaches a quasi-thermal equilibrium state in a shorter time for NBI#2 as compared with that for NBI#1, which indicates that the neutron generation is dominated by the lower energy deuterons, i.e. knock-on tail.

In general slowing-down process of fast-ion ion, the peak of fast-ion distribution function slows down relatively slower at the initial state. When the lower energy side of the distribution function approaches the thermal energy range of background particles, the bulk component of the distribution function immediately increases, and the slowing-down speed becomes faster. When the most part of the distribution function approaches the thermal energy range, the influence of the up-scattering begins to be appreciable, and the slowing-down speed is further relaxed. So, the neutron decay time (slowing-down speed) is not constant during the

slowing-down process (in actual plasma the effect of particle loss may make the phenomena further complicate). It should be noted that the neutron decay process (shape of the decay line) does not depend on the intensity of the beam tails (does not depend on the fraction of the deuterium impurity). Thus, if the attenuation property was different, it would indicate that the shape of the distribution function is different. In simulations, the intersect point of two curves in **Fig.3** can change depending on the plasma parameter. For example, if the density increases (decreases), the slowing-down of fast ions are fastened (delayed) and the two curves intersect faster (later). Nevertheless, the relative tendency between two curves does not change regardless plasma parameters. It should be noted that we do not examine the neutron decay time directly, but instead focus our attention on the difference in the shape of the decay curves by extending the concerned time duration. The observed tendency is robust, because a similar tendency was observed in all the shots in the LHD experiments, even if NBI#3 was used instead of NBI#1.

3.2 Observation of NES effect on the neutron decay time

We further ascertain the knock-on effect due to NES. For this purpose, the neutron decay times of the neutrons that were produced by the $D(d,n)^3He$ reactions between the injected beam and the bulk deuterons were measured right after NBI#4 and 5 (vertical injections, 100% deuterium) were terminated. The neutron decay times were compared for cases in which any one of the tangential beams NBI#1, 2, or 3 was continuously injected during the slowing-down process and in which no tangential beams were injected. In this case, since NBI#4 and 5 (100% deuterium) is used, knock-on tail itself is completely buried under the beam deuterons. However, we expected that if NBI#1, 2, or 3 were continuously injected during the neutron decay process, since the bulk and beam deuterons are scattered into higher energy range via NES, the neutron decay process is predicted to be delayed.

During the experiment, deuterium plasma is prepared by ECH and neutral-beam (100% deuterium NBI#4 and 5) heating. After 4.01 s from initiating the plasma discharge, deuterium beam injections (NBI#4 and 5) were terminated. We then focused on the investigation of the

neutron decay processes produced by the D(d,n)^{3}He reactions with the ~60-KeV deuterium beams (NBI#4 and 5) and bulk deuterons after 4.01 s. In **Fig. 6**, the time variations of the neutron generation rates with and without additional H-beam heating (NBI#1) are plotted. Without H-beam heating, the plasma density (temperature) was approximately 30 (20)% lower (higher) compared with the beam-injected case. If the fast-ion slowing-down time τ_s obeys the theoretical scaling, i.e., $\tau_s \propto T_e^{3/2}/n_e$, the neutron attenuation can be faster in low-temperature and high-density plasma. The decay curves show that the neutron decay time becomes shorter when H beam is not injected contrary to the plasma condition. The energetic protons might weaken the deuterons slowing-down process via NES. For 18 shots, the neutron decay times τ_n observed in experiment (defined as the time after which the neutron generation rate falls to $1/e$ after NBI#4 and 5 are terminated) are plotted as a function of the neutron decay time predicted by the FP simulations τ_{FP} (evaluated as the time after which the beam-thermal D(d,n)^{3}He reaction rate is reduced to $1/e$ in the simulation). The results are presented in **Fig. 7** and are compared with the simulations using the BFP model [2, 3]. In the simulations we assumed uniform plasma, and measured temperature and density were taken for each of the shots. We chose the temperature and density at $a/2$ (where a is the minor radius), because the most part of the neutrons is carried around this region. In the FP and BFP simulations the beam injection energy and power are chosen as 180 (60) keV and 6 (4) MW for hydrogen (deuterium) beam. The confinement times for protons and deuterons are taken from the work of Nuga, et al. [16,17] as 0.5 and 0.03 s respectively. The squares represent the experimental results with (red) and without (black) H beams (NBI#1, 2, or 3), whereas the circles represent the BFP simulations with (red) and without (black) H beams. The green circles represent the FP simulation when we only consider the Coulomb scattering process (the green circles are on the diagonal line). When we only consider the Coulomb scattering process, the neutron decay times increase compared with the cases when no H beam is injected (black circles and squares). This is due to the energy transfer from protons to deuterons via many small-angle scatterings. We further observe that the neutron decay times

when additional H-beam injection is made (red circles and squares) are larger compared to those when only the Coulomb scattering is considered. For 5 experimental shots that presented by red squares (within a large dotted circle), the NBI powers were 20~30 % smaller compared with the other upper 7 red squares. We guess that if the NBI powers for the 5 shots were the same level with other 7 shots, the knock-on effect would be enhanced, and the neutron decay times would approach other 7 shots with H-beam heating. The result indicates that the H beam adds energy to the slowing-down component via other process, i.e., NES, in addition to the Coulomb scattering, so that the decay process of the neutrons is further delayed.

4. Conclusion

The deuteron slowing-down behaviour in a fusion plasma has been experimentally shown to likely be affected by the NES caused by energetic protons. NES increases the amount of energy passed from fast ions to plasma background ions, with respect to the Coulomb-only case which heats also plasma background electrons. The NES effect would further increase as the ion energy increasing [2,3]. The observations reported in this paper show an experimental technique that can be used in future experiments to probe directly the deuteron slowing down in burning plasmas. In our FP and BFP simulations, several parameters are necessary to reproduce experimentally obtained data, e.g. confinement times, however, the analysis would still be useful to understand the property of the NES effect. For more detailed qualitative analysis, more sophisticated simulation code which can consistently determine the plasma parameters would be required.

Acknowledgement

The authors would like to thank the cooperative program of NIFS 17KLPH029 and the LHD experimental team for their contribution. The first author is grateful to Emer. Prof. Y. Nakao for long years of discussion and encouragement.

References

[1] Devany J. J., Stein M. L., Nucl. Sci. Eng. **46**, 323 (1971).

[2] Matsuura H., Nakao Y., Phys. Plasmas **13**, 062507 (2006).

[3] Matsuura H., Nakao Y., Plasma Phys. Contr. Fusion **53**, 035023 (2011).

[4] Ballabio L., Gorini G., Källne J., Phys. Rev. E **55**, 335(1997).

[5] Ryutov D., Phys. Scr. **45**, 153 (1992).

[6] Fisher R. K., Rev. Sci. Inst. **10**, 3556 (2004).

[7] Källne J., Ballabio L., Frenje J., *et al*., Phys. Rev. Lett. **85**, 1246 (2000).

[8] Korotkov A. A., Gondhalekar A., Akers R. J., Phys. Plasmas **7**, 957 (2000).

[9] Galambos J., Gilligan J., Grrenspan E., *et al*., Nucl. Fusion **24**, 739 (1984).

[10] Nakao Y., Hori H., Hanada T., *et al*., Nucl. Fusion **28**, 1029 (1988).

[11] Osakabe M., Isobe M., Tanaka M., *et al*., IEEE Trans. Plasma Sci. **46**, 2324 (2018).

[12] Perkins S. T., Cullen D. E., Nucl. Sci. Eng. **77**, 20 (1981).

[13] Bosch H. S., Hale G. M., Nucl. Fusion **32**, 611 (1992).

[14] Honma M., Murakami S., Nuga H., *et al*., Plasma Fusion Res. **11**, 2403109 (2016).

[15] Isobe M., Ogawa K., Nishitani T., *et al*., Nucl. Fusion **58**, 082004 (2018).

[16] Nuga H., Seki R., Ogawa K., *et al*., Plasma Fusion Res. **14**, 3402075 (2019).

[17] Nuga H., Seki R., Kamio S., *et al*., Nucl. Fusion **59**, 016007 (2019).

Table 1　The beam species, D containment fraction, normal rated power and energy of NBIs in LHD (see Fig.1)

NBI No.	Species	D containment	P_{NBI} [MW]	E_{NBI} [keV]
NBI#1	Hydrogen	~1% D	5.0	180.0
NBI#2	Hydrogen	N/A D	5.0	180.0
NBI#3	Hydrogen	~1% D	5.0	180.0
NBI#4	Duterium	100% D	9.0	60.0
NBI#5	Deutrium	100% D	9.0	80.0

Figure 1 H. Matsuura, et al.

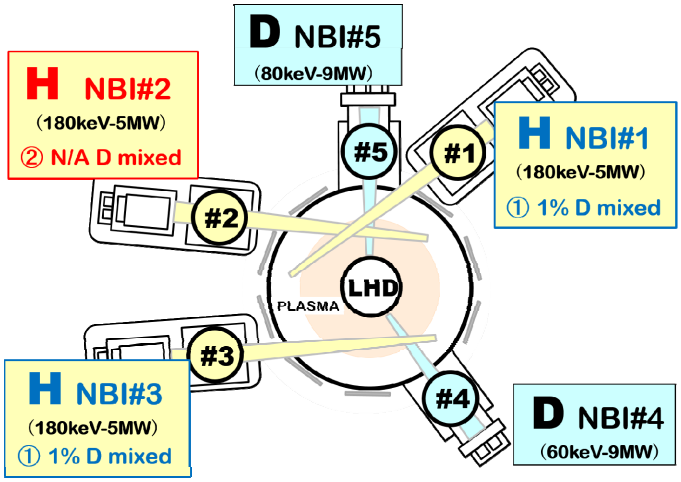

Fig. 1 Schematic of the NBI systems around the LHD.

Figure 2 H. Matsuura, et al.

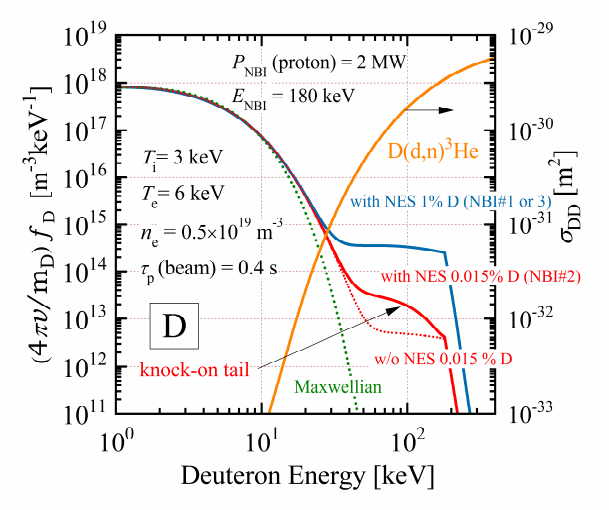

Fig. 2 Equilibrium deuteron distribution functions with a beam-created (NBI#1 or 3) or knock-on (NBI#2) tail (evaluated on the basis of BFP simulations [2, 3]) for T_e = 6 keV, T_i = 3 keV, n_e = 0.5×10^{19} m^{-3} along with the D(d,n)^{3}He fusion cross-section.

Figure 3 H. Matsuura, et al.

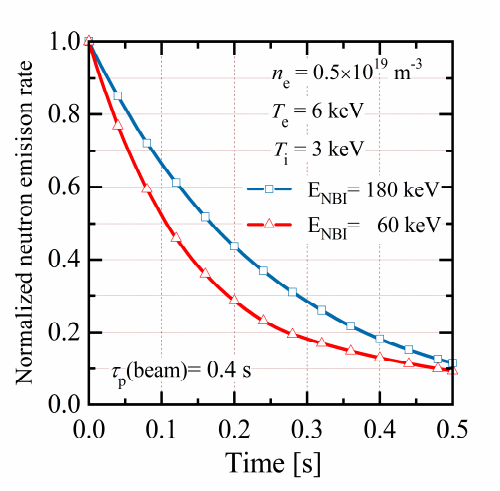

Fig. 3 Difference in normalized neutron generation rates after the NBIs were terminated for beam-injection energy (E_{NBI}) of 180 and 60 keV. T_e = 6 keV, T_i = 3 keV, n_e = 0.5×10^{19} m^{-3}, and τ_p for energetic deuteron = 0.4 s are assumed.

Figure 4 H. Matsuura, et al.

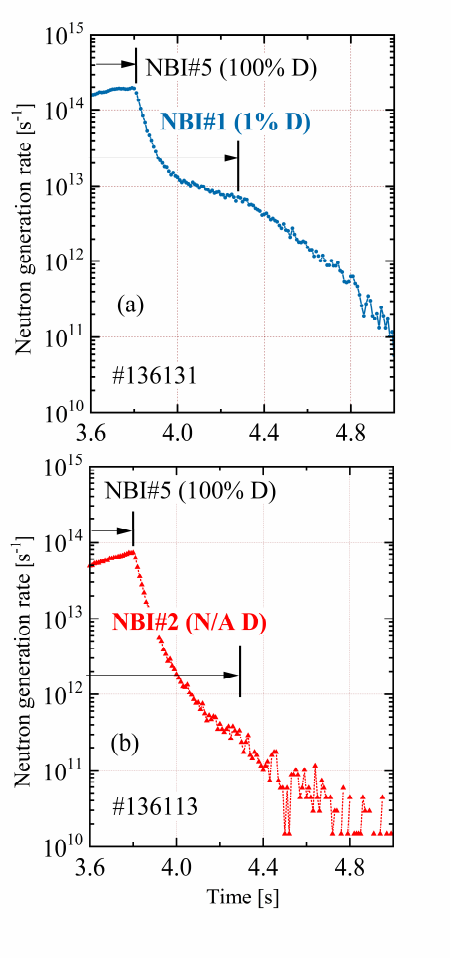

Fig. 4 Decay process of the neutron-generation rate after the NBIs were terminated (NBI#5 was terminated at 3.8 s, and (a) NBI#1 or (b) NBI#2 was terminated at 4.3 s from the beginning of plasma discharge).

Figure 5 H. Matsuura, et al.

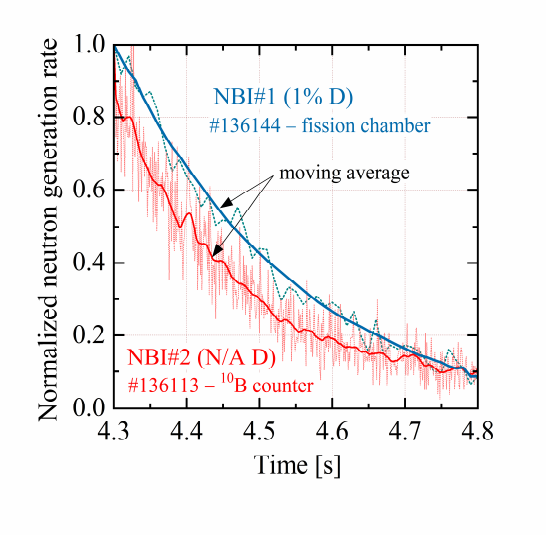

Fig. 5 Decay processes of the normalized neutron generation rates after 4.3 s for NBI#1 (1% deuterium contained: #136144) and NBI#2 (N/A deuterium contained: #136113).

Figure 6 H. Matsuura, et al.

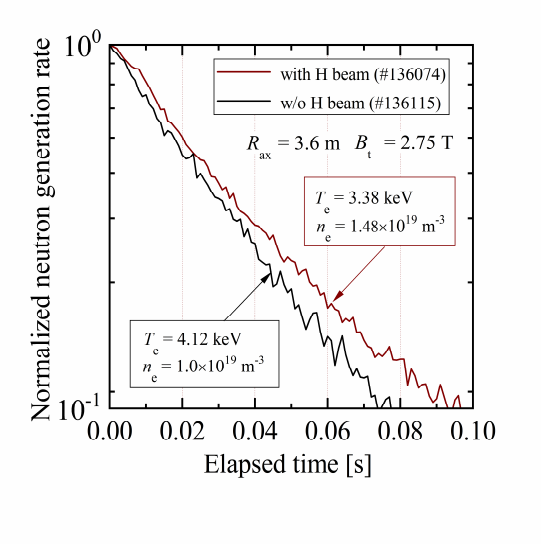

Fig. 6 Decay processes of the normalized neutron generation rates with (red) and without (black) NBI#1 heating.

Figure 7 H. Matsuura, et al.

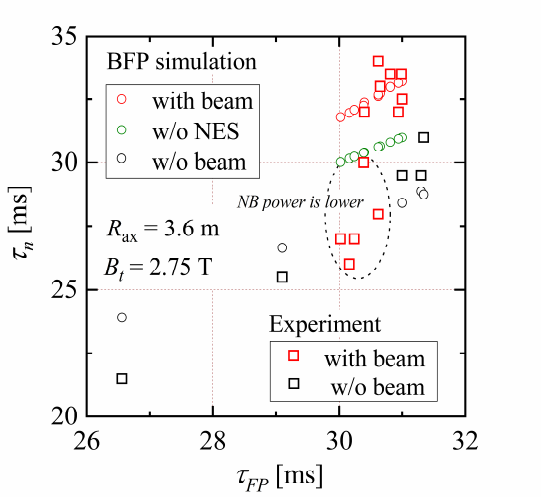

Fig. 7 Neutron decay time τ_n vs. τ_{FP} for 18 shots with additional NBI#1, 2, or 3 being adopted continuously during the neutron decay process (red squares) along with the results for no additional H beam injection (black squares) after NBI#4 and 5 were terminated. The circles represent the neutron decay time evaluated by the BFP simulations with (red circles) and without (black circles) H beam along with the FP simulation when only Coulomb scattering is considered (green circles).